Fast beam-ion instability II. Effect of ion decoherence

G. V. Stupakov, T. O. Raubenheimer, and F. Zimmermann

Stanford Linear Accelerator Center, Stanford University, P.O. Box 4349, Stanford, California 94309

The ionization of residual gas by an electron beam in an accelerator generates ions that can resonantly couple to the beam through a wave propagating in the beam-ion system. A beam-ion instability is studied for a multibunch train, taking into account the decoherence of ion oscillations due to the ion frequency spread. It is shown that while the decoherence does not completely suppress the instability, it makes the growth rate smaller. A comparison of analytical and numerical results indicates good agreement with direct macroparticle simulation of the instability.

I. INTRODUCTION

A fast beam-ion instability, which is caused by the interaction of a single-electron-bunch train with the residual gas ions, has been studied recently in Ref. [1]. The instability mechanism is the same in both linear accelerators and storage rings assuming that the ions are not trapped from turn to turn. The ions generated by the head of the bunch train oscillate in the transverse direction and resonantly interact with the betatron oscillations of the subsequent bunches, causing the growth of the initial perturbation of the beam. The model employed in Ref. [1] treated all ions as oscillating with the same frequency equal to the frequency of small-amplitude oscillations of the ion centroid in the potential well of the beam. In reality, there are several sources that cause a frequency spread within the ion population. It is known that inclusion of the frequency spread and the decoherence associated with it in an instability problem usually results in the Landau damping effect and in some situations can suppress the instability.

A study of this effect for the fast ion instability is presented in this paper. To find the solution of the equations describing the instability with ion decoherence, we developed an approach that differs from that of Ref. [1] and is based on the averaging over the fast ion and electron oscillations. We show that although the ion frequency spread does not fully suppress the instability, it decreases the growth rate, making it in a typical situation two or three times smaller than that predicted in Ref. [1]. For the sake of simplicity, we focus on the interaction of an electron beam with ions, although similar effects apply to a positron beam trapping free electrons.

The variation of the ion frequency ω_i included in this paper is caused by two sources. One of them is due to the horizontal beam density profile in a flat beam, which causes the local ion frequency to depend on the horizontal position. Another source of spread in ω_i is the nonlinearity of the ion oscillations inside the beam.

For analytical study we adopt a model that treats the bunch train as a continuous beam. This model is applicable if the distance between the bunches l_b is smaller than the betatron wavelength $l_b \ll c/\omega_\beta$ and the ion oscilla-

tion wavelength $l_b \ll c/\omega_i$. This condition is well satisfied for multibunch machines such as the PEP-II High Energy Ring (HER) [2] or the Damping Ring of a SLAC design for a future linear collider (NLC) [3]. As in Ref. [1], we assume a one-dimensional model that treats only vertical linear oscillation of the centroids of the beam and the ions.

The paper is structured as follows. In Sec. II, the differential equations of motion are derived. Sec. III discusses averaging of the equations based on different time scales associated with oscillations and growth of the instability. The ion frequency spread and resulting decoherence of ion oscillations are analyzed in Sec. IV. Analytical and numerical solutions of the equations for the NLC Damping Ring and PEP-II High Energy Ring are presented in Secs. V and VI, respectively. They are compared with direct computer simulation of the instability in Sec. VII and the results are summarized in Sec. VIII.

II. EQUATIONS OF MOTION

We will assume a rigid vertical motion of the beam and define the offset of the centroid at time t and longitudinal position s as $y_b(s,t)$. The distance s is measured from the injection point at $t = 0$. The equation for the beam centroid, including the interaction with the ion background, is

$$\left(\frac{1}{c}\frac{\partial}{\partial t} + \frac{\partial}{\partial s}\right)^2 y_b(s,t) + \frac{\omega_\beta^2}{c^2} y_b(s,t)$$

$$= \kappa(ct - s)[y_i(s,t) - y_b(s,t)] . \quad (1)$$

The left-hand side of this equation accounts for the free betatron oscillation of a moving beam (we assume $v_{\text{beam}} \approx c$). On the right-hand side, we included the force acting on the beam from the ions whose centroid is offset by $y_i(s,t)$. In the linear theory, this force is proportional to both the relative displacement between the beam and ions centroids and the ion density. Assuming a continuous electron beam with a uniform density per unit length, the ion density increases due to collisional ionization as $ct - s$ (it is equal to zero before the beam

head arrives at the point s at time $t = s/c$). After separating the factor $ct - s$ on the right-hand side of Eq. (1), the coefficient κ is (see Ref. [1] for details in which the factor K is related to our κ through the relation $K = \kappa l$, where l is the length of the bunch train)

$$\kappa \equiv \frac{4\dot{\lambda}_{\text{ion}} r_e}{3\gamma c \sigma_y (\sigma_x + \sigma_y)} , \qquad (2)$$

where γ denotes the relativistic factor for the beam, r_e is the classical electron radius, $\sigma_{x,y}$ denotes the horizontal and the vertical rms beam size, respectively, and $\dot{\lambda}_{\text{ion}}$ is the number of ions per meter generated by the beam per unit time. Assuming a cross section for collisional ionization of about 2 Mb (corresponding to carbon monoxide at 40 GeV), we have

$$\dot{\lambda}_{\text{ion}}(\text{m}^{-1}\,\text{s}^{-1}) \approx 1.8 \times 10^9 n_e(\text{m}^{-1}) p_{\text{gas}}(\text{Torr}) , \qquad (3)$$

where n_e is the number of electrons in the beam per meter and p_{gas} the residual gas pressure in torr.

To find the equation for ions, we will assume that they perform linear oscillations inside the beam with a frequency ω_i. Furthermore, we will allow a continuous spectrum of ω_i given by a distribution function $f(\omega_i)$ normalized so that

$$\int f(\omega_i)\, d\omega_i = 1 . \qquad (4)$$

The spread in ω_i at a given position s (and for a given ion species) is caused by several sources; they are discussed in more detail in Sec. IV. The distribution $f(\omega_i)$ is peaked around the frequency $\omega_i = \omega_{i0}$ corresponding to small vertical oscillations on the axis

$$\omega_{i0} \equiv \left[\frac{4n_e r_p c^2}{3A\sigma_y (\sigma_x + \sigma_y)} \right]^{1/2} , \qquad (5)$$

where A designates the atomic mass number of the ions, n_e the number of electrons in the beam per unit length, and r_p the classical proton radius ($r_p \approx 1.5 \times 10^{-16}$ cm). Typically, the frequency spread $\Delta\omega_i$ is not large; we assume $\Delta\omega_i \ll \omega_{i0}$.

We also have to distinguish between the ions generated at different times t' because they will have an initial offset equal to the beam coordinate $y_b(s, t')$. Let us denote by $\tilde{y}_i(s, t|t', \omega_i)$ the displacement, at time t and position s, of the ions generated at t' ($t' \leq t$) and oscillating with the frequency ω_i. We have an oscillator equation for $\tilde{y}_i$

$$\frac{\partial^2}{\partial t^2} \tilde{y}_i(s, t|t', \omega_i) + \omega_i^2 [\tilde{y}_i(s, t|t', \omega_i) - y_b(s, t)] = 0 , \qquad (6)$$

with the initial condition

$$\tilde{y}_i(s, t'|t', \omega_i) = y_b(s, t') , \qquad \left. \frac{\partial \tilde{y}_i}{\partial t} \right|_{t=t'} = 0 . \qquad (7)$$

Finally, averaging displacement of the ions produced at different times t' and having different frequencies ω_i gives the ion centroid $y_i(s, t)$

$$y_i(s, t) = \frac{1}{t - s/c} \int_{s/c}^t dt' \int d\omega_i f(\omega_i) \tilde{y}_i(s, t|t', \omega_i) . \qquad (8)$$

Equations (1) and (6)–(8) constitute a full set of equations governing the development of the instability in the beam-ion interaction.

III. AVERAGING OF THE EQUATIONS

Equation (6) can be easily integrated with the initial conditions (7) yielding

$$\tilde{y}_i(s, t|t', \omega_i) = y_b(s, t) - \int_{t'}^t \frac{\partial y_b(s, t'')}{\partial t''}$$
$$\times \cos \omega_i(t - t'')\, dt'' . \qquad (9)$$

Now using Eq. (8), Eq. (1) reduces to an integrodifferential equation

$$\left(\frac{1}{c} \frac{\partial}{\partial t} + \frac{\partial}{\partial s} \right)^2 y_b(s, t) + \frac{\omega_\beta^2}{c^2} y_b(s, t)$$

$$= -\kappa \int_{s/c}^t (ct' - s) \frac{\partial y_b(s, t')}{\partial t'} D(t - t')\, dt' , \qquad (10)$$

where $D(t - t')$ denotes a decoherence function defined as

$$D(t - t') = \int d\omega_i \cos \omega_i(t - t') f(\omega_i) . \qquad (11)$$

This function represents the oscillation of the centroid of an ensemble of ions with a given frequency distribution $f(\omega_i)$ having an initial unit offset.

Instead of t and s, it is convenient to transform to independent variables z and s, where $z = ct - s$. The variable z measures the distance from the head of the beam train and for a fixed z the variable s plays a role of time. Denoting

$$y(s, z) \equiv y_b(s, s + z) , \qquad (12)$$

Eq. (10) takes the form

$$\frac{\partial^2}{\partial s^2} y(s, z) + \frac{\omega_\beta^2}{c^2} y(s, z)$$

$$= -\kappa \int_0^z z' \frac{\partial y(s, z')}{\partial z'} D(z - z')\, dz' . \qquad (13)$$

If $D(z) = \cos \omega_i z$ (no frequency spread), Eq. (13) reduces to the equation derived in Ref. [1].

We will assume that the interaction between the beam and the ions is small

$$c^2 \kappa l \ll \omega_{i0}^2, \omega_\beta^2 , \qquad (14)$$

where l denotes the length of the bunch train, so that the instability develops on a time scale that is much larger

than both the betatron period and the period of ion oscillations. Typically this inequality is easily satisfied. In such a situation, the most unstable solution of Eq. (13) can be represented as a wave propagating in the beam with a slowly varying amplitude and phase

$$y(s,z) = \mathrm{Re} A(s,z) e^{-i\omega_\beta s/c + i\omega_{i0} z/c} ,$$ (15)

where the complex amplitude $A(s,z)$ is a "slow" function of its variables

$$\left| \frac{\partial \ln A}{\partial s} \right| \ll \frac{\omega_\beta}{c} , \quad \left| \frac{\partial \ln A}{\partial z} \right| \ll \frac{\omega_{i0}}{c} .$$ (16)

For a fixed z, the s dependence of Eq. (15) describes a pure betatron oscillation, while, for a fixed s (that is, in the ion frame of rest), the z-dependent part implies oscillations with the frequency ω_{i0}. Hence the wave resonantly couples the ions and the electrons. Substituting Eq. (15) into Eq. (13) and averaging it over the rapid oscillations with the frequencies ω_{i0} and ω_β, one finds

$$\frac{\partial A(s,z)}{\partial s} = \frac{\kappa \omega_{i0}}{4\omega_\beta} \int_0^z z' A(s,z') \hat{D}(z-z') dz' ,$$ (17)

where the function $\hat{D}(z)$ is

$$\hat{D}(z) = \int d\omega_i f(\omega_i) e^{i(\omega_i - \omega_{i0}) z/c} .$$ (18)

One of the advantages of the above approach is that it allows a simple scaling of the instability with the vacuum pressure. Indeed, the only place where the pressure p enters Eq. (17) is the parameter κ, which is proportional to p [see Eqs. (2) and (3)]. By introducing a variable $s\kappa$ instead of s, we can eliminate κ from the equation. This means that increasing the pressure n times is equivalent to the shrinking the s axis by the same factor. Thus, having solved Eq. (17) for one particular value of pressure, we can use the result for various p by simply rescaling the s variable $s \propto p^{-1}$.

IV. ION DECOHERENCE

The frequency spread of the ions at a given longitudinal coordinate s stems from several sources. One of them is a variation of the electron density in the beam along the horizontal axis. Since the ion frequency scales as the square root of the electron density $\omega_i \propto \sqrt{n_e}$, ions located at different coordinates x in a flat beam will have different ω_i. For a Gaussian distribution of electrons in x, $n_e \propto \exp(-x^2/2\sigma_x^2)$ and we obtain $\omega_i(x) \propto \exp(-x^2/4\sigma_x^2)$. Hence

$$\omega_i(x) - \omega_{i0} = \omega_{i0} \left[\exp(-x^2/4\sigma_x^2) - 1 \right] ,$$ (19)

where ω_{i0} is the frequency at $x=0$.

To find the decoherence function $\hat{D}$, we will utilize a simple one-dimensional model that assumes that the ion frequency of horizontal oscillations is much smaller than the vertical frequency ω_i and neglects the horizontal ion

motion on the time scale of the decoherence. In this model, the ion distribution in x is the same as the electron distribution (because the rate of ionization is proportional to n_e)

$$f_i(x) = \frac{1}{\sqrt{2\pi}\sigma_x} \exp\left(-x^2/2\sigma_x^2\right)$$ (20)

and Eq. (18) takes the form

$$\hat{D}(t) = \int_{-\infty}^{\infty} dx f_i(x) \exp\{-i\omega_{i0} t [1 - \exp(-x^2/4\sigma_x^2)]\}.$$ (21)

Note that in this model we overestimate the effect of the decoherence. For flat beams, a typical ratio of the horizontal and vertical oscillation frequencies is roughly 3. Thus the horizontal motion of the ions modulates the vertical oscillation frequency ω_i between ω_{i0} and $\omega_i(x)$, making the average ω_i smaller than $\omega_i(x)$. To fully account for this effect, one has to deal with the two-dimensional ion motion, which would make the consideration much more involved.

At this point, we note that Eq. (21) has been defined as the average offset of the ions at a given s. However, the quantity relevant to the electron-ion coupling is the average force that acts on the electron beam. The force differs from the average displacement because the ion density decreases with x and thus the ion electric field at the beam edges is suppressed relative to that at the bunch center. To account for this effect, we correct $\hat{D}(t)$ by including the electron density n_e in the integrand of Eq. (21)

$$\hat{D}(t) = \mathrm{const} \int_{-\infty}^{\infty} dx f_i(x) n_e(x)$$
$$\times \exp[-i\omega_{i0} t(1 - e^{-x^2/4\sigma_x^2})] ,$$ (22)

where the constant in Eq. (22) must be chosen such that $\hat{D}(0) = 1$. This gives

$$\hat{D}(t) = \frac{1}{\sqrt{\pi}\sigma_x} \int_{-\infty}^{\infty} dx \exp[-i\omega_{i0} t(1 - e^{-x^2/4\sigma_x^2})$$
$$-x^2/\sigma_x^2].$$ (23)

The plots of the real and imaginary parts of this function are shown in Fig. 1. Asymptotically, for large values of $\omega_{i0} t$,

$$\hat{D}(t) \approx (1 + i\alpha\omega_{i0} t)^{-1/2} ,$$ (24)

where the numerical factor $\alpha = 1/4$.

Another source of ion decoherence is the nonlinearity of the electron potential. It results in a dependence of ω_i on the amplitude of the oscillation and causes an additional spread in the oscillation frequencies ω_i. We have numerically computed the decoherence function due to nonlinearity in a manner similar to the approach of Ref. [4]; it is also plotted in Fig. 1. One can show that the decoherence due to nonlinearity has the same asymptotes as
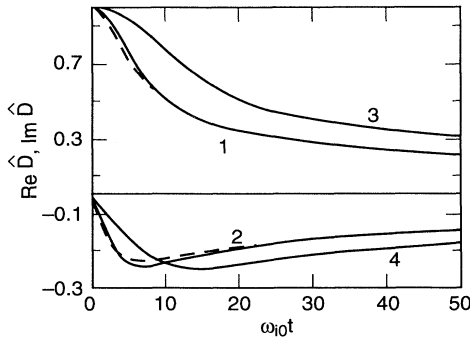
FIG. 1. Real (curve 1) and imaginary (curve 2) parts of the function $\hat{D}(t)$ given by Eq. (23) and the asymptotes of Eq. (24) (dashed lines). Curves 3 and 4 shows real and imaginary parts, respectively, of the decoherence function due to nonlinearity of the ion motion.

Eq. (24) with a somewhat smaller α. In what follows, we will use the simple form given by Eq. (24) for $\hat{D}(t)$ in which we set $\alpha = 3/8$ to account for the additional decoherence due to the nonlinearity.

Finally, concluding this section, we mention a simple model of decoherence that assumes an exponential behavior of $\hat{D}(t)$

$$\hat{D}(t) = e^{-\omega_{i0}t/2Q_i} , \qquad (25)$$

where Q_i is the quality factor of ion oscillations. Choosing Q_i so that Eq. (25) fits the $|\hat{D}(t)|$ given by Eq. (23) for $0 < \omega_{i0}t < 50$, we find $Q_i \approx 16$. This model strongly overestimates damping for large t, but it allows an analytical solution for the instability, as we will show in the next section.

V. ANALYSIS

Let us for a moment ignore the ion decoherence in Eq. (17) and set $\hat{D}(z) \equiv 1$. In this case, the equation can easily be solved analytically. Differentiation with respect to z reduces Eq. (17) to the differential equation

$$\frac{\partial^2 A(s,z)}{\partial s \partial z} = \frac{\kappa \omega_{i0}}{4\omega_\beta} z A(s,z) . \qquad (26)$$

For the initial condition $A(0,z) = 1$, the solution is

$$A(s,z) = I_0 \left(z\sqrt{\frac{\kappa \omega_{i0}}{2\omega_\beta} s} \right) , \qquad (27)$$

where I_0 is the zeroth-order Bessel function of imaginary argument. This solution was found in Ref. [1] using a different method. For large values of the argument the asymptotic expansion of the Bessel function yields

$$A(s,z) \approx \left(2\pi z\sqrt{\kappa \omega_{i0}s/2\omega_\beta} \right)^{-1/2}$$
$$\times \exp\left(z\sqrt{\kappa \omega_{i0}s/2\omega_\beta} \right) , \qquad (28)$$

which indicates an instability with a characteristic time $\tau \approx 2\omega_\beta/\kappa \omega_{i0}l^2 c$, where l is the length of the bunch train. Note that since $A(s,z) \propto \exp\left(z/l\sqrt{s/c\tau} \right)$, the characteristic time τ does not represent an e-folding time and the instability develops much slower than it would in the case of normal exponential growth $\propto \exp(s/c\tau)$.

Equation (17) can be also solved analytically using the decoherence function given by Eq. (25). In this case, differentiating Eq. (17) with respect to z yields

$$\frac{\partial^2 A(s,z)}{\partial s \partial z} = \frac{1}{2c\tau l^2} z A(s,z) - \gamma \frac{\partial A(s,z)}{\partial s} , \qquad (29)$$

where $\gamma = \omega_{i0}/2Q_i c$. A solution to this equation with the initial condition $A(0,z) = 1$ is

$$A(s,z) = \exp(-\gamma z) I_0 \left(\frac{z}{l}\sqrt{\frac{s}{c\tau}} \right)$$
$$+ \gamma \int_0^z dz' I_0 \left(\left[\frac{s(z^2 - z'^2)}{c\tau l^2} \right]^{1/2} \right)$$
$$\times \exp\left[-\gamma(z - z') \right] . \qquad (30)$$

Using the asymptotic form for the Bessel function, one can show that for large s

$$A(s,z) \approx \left(2\pi \frac{z}{l}\sqrt{\frac{s}{c\tau}} \right)^{-1/2} \exp\left(\frac{z}{l}\sqrt{\frac{s}{c\tau}} - \gamma z \right)$$
$$\times \left[1 + \left(\frac{\pi z l \gamma^2}{2}\sqrt{\frac{c\tau}{s}} \right)^{1/2} \right.$$
$$\left. \times \exp\left(\frac{1}{2} z l \gamma^2 \sqrt{\frac{c\tau}{s}} \right) \right] . \qquad (31)$$

Equation (31) indicates that while the strong exponential damping due to decoherence does not suppress the instability, it makes the effect much weaker at the tail of a long bunch train. For very large times s, Eq. (31) approaches Eq. (28), except for an s-independent amplitude reduction by $\exp(-\gamma z)$. In this model, the ultimate growth is unchanged by the decoherence, but this is only valid after exceedingly long times and is not interesting for practical cases.

VI. NUMERICAL RESULTS

To study the effect of the decoherence in more realistic cases, we wrote a computer code that numerically integrates Eq. (17) with $\hat{D}(t)$ given by Eq. (24). The two input parameters for the code are the characteristic time $\tau = 2\omega_\beta/\kappa \omega_{i0}l^2 c$ and the train length $\omega_{i0}l/c$.

Simulations have been performed for the NLC Damp-

ing Ring and the PEP-II HER. In the NLC Damping Ring (see relevant parameters in Ref. [1]), we assumed a residual gas with a vacuum pressure of $p = 10^{-8}$ Torr and an atomic number of $A=28$. This corresponds to a characteristic time of $\tau = 45$ ns and a bunch length of $\omega_{i0}l/c = 150$. The results are depicted in Fig. 2 for the initial condition $A(0,z) = 1$; for comparison, in Fig. 3, we plot the solution of Eq. (27) for the same parameters but without the decoherence. The plots show the growth of the beam centroid at ten positions evenly spaced along the bunch train. Comparing Figs. 2 and 3 shows the decoherence slowing down the instability. To characterize the growth rate of the instability, we defined τ_{growth} as an e-folding time for the last bunch in the train. Since the instability is not exponential, τ_{growth} varies with time. For the time interval 1 μs $< t < 2$ μs, we find that $\tau_{growth} \approx 0.5$ μs without decoherence and $\tau_{growth} \approx 1$ μs with ion decoherence; the decoherence decreases the growth rate by a factor 2.

Figures 2 and 3 illustrate the growth of the instability from an initial condition Eq. (15), which is the most unstable perturbation. In reality, the initial noise in the beam will contain different harmonics of which only one or two, having a spatial period $2\pi c/\omega_{i0}$, are very unstable. Assuming that the number of bunches in the train equals N_b and their displacements are uncorrelated with the rms value of δ, a simple statistical argument shows that the amplitude of harmonics in the bunch will be of the order of $\delta/\sqrt{N_b}$. To illustrate the effect of random initial positions, we integrated Eq. (17) including the effect of the ion decoherence with the initial condition corresponding to uncorrelated displacement with $\delta = 1$ for 90 bunches in the NLC Damping Ring. The result is shown in Fig. 4 for $p = 10^{-9}$ and $p = 10^{-8}$ (as noted in Sec. III, variation of the pressure simply rescales the horizontal axis in the plot). The figure shows that the development of the instability is somewhat delayed until the amplitude of the unstable mode with an initial value $\delta/\sqrt{90} \approx 0.1$ reaches a value comparable to 1; for $p = 10^{-8}$, this occurs after roughly 5 μs. After this point, the growth proceeds at about the same rate as in Fig. 2.

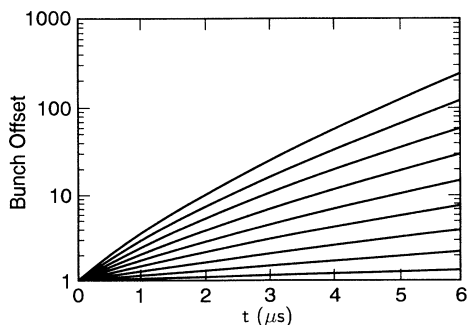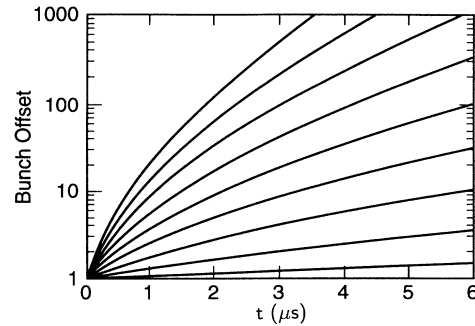For the PEP-II High Energy Ring, we assumed a vac-

FIG. 3. Growth of an initial unit offset in the NLC Damping Ring at ten different points in the train (the line corresponding to the first point is superimposed on the abscissa) without decoherence.

uum pressure of $p = 10^{-9}$ Torr and $A=28$. This corresponds to a characteristic time $\tau = 5.5$ μs and a bunch length $\omega_{i0}l/c = 220$. The bunch offsets at ten positions in the train are shown in Fig. 5 as a function of s for the initial condition $A(0,z) = 1$. From this figure, we estimate that the e-folding growth time, on the time interval 200 μs $< t < 400$ μs, is roughly $\tau_{growth} \approx 150$ μs. As noted before, this growth time depends on the interval considered.

VII. COMPUTER SIMULATIONS

We also performed direct macroparticle simulations of the instability using a computer code described in Ref. [1]. In the simulations, each of the bunches is represented by 10 000 macroparticles and they interact with the ions, which are represented by roughly 50 000 macroparticles. In this manner, the beam and ion distributions evolve self-consistently as the beam is tracked through the magnet lattice.

FIG. 2. Growth of an initial unit offset in the NLC Damping Ring at ten different points in the train (the line corresponding to the first point is superimposed on the abscissa) with ion decoherence.
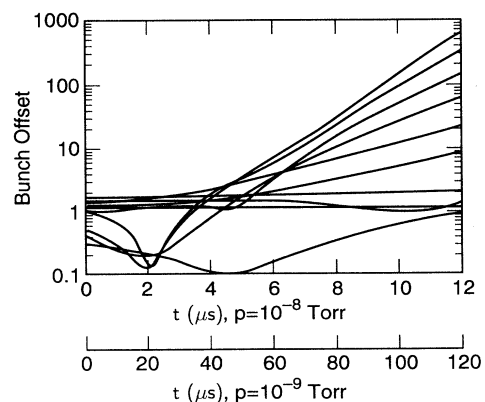

FIG. 4. Instability in the NLC Damping Ring with random initial condition and with ion decoherence.
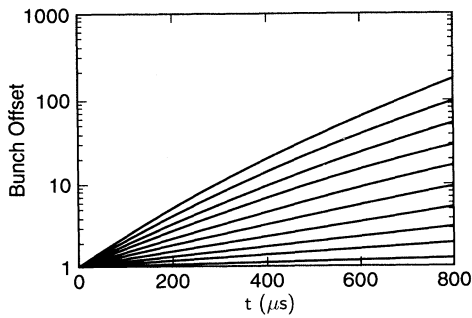
FIG. 5. Growth of an initial unit offset in the PEP-II High Energy Ring.

FIG. 6. Macroparticle simulation of the instability in the NLC Damping Ring with a vacuum pressure of 10^{-8} Torr and $A=28$; the position of every tenth bunch is plotted.

The results of a simulation for the NLC Damping Ring with a vacuum pressure of $p = 10^{-8}$ Torr are shown in Fig. 6, where we have plotted the oscillation amplitude, normalized by $\sqrt{N_{\mathrm{macro}}}/\sigma_y$; this allows for a direct comparison with Fig. 4. Comparing Fig. 6 with Fig. 4 shows good agreement for the growth rate of the instability during the initial stage ($t < 6$ μs). At later times, the macroparticle simulation exhibits saturation, which is presumably due to the nonlinearity of the beam-ion force as the amplitude of the oscillations become comparable to the rms beam size σ_y; this occurs at a value of 100 in the normalized units of the plot.

VIII. DISCUSSION

In this paper we have studied the effect of the ion frequency spread on the development of the beam-ion instability. We have considered variations of the ion frequency due to the nonlinearity of the beam-ion force in both x and y planes. In general, the dependence of ω_i on the horizontal motion is the more important effect and should strictly be described with a two-dimensional treatment of the ion motion. There are other sources of ion frequency spread that we have not considered, although they can be included in our formalism in a straightforward manner. In particular, the ion frequency will change as the β functions and beam sizes in the optical lattice vary through a cell. This is not a very important effect in a FODO lattice, but it could prove to be much more significant in other lattices such as the triple bend achromat or Chasman-Green structures used in many synchrotron light sources.

In all cases, the variation of the ion frequency causes Landau damping and slows the instability growth rate. In the two examples that we studied, the growth rate was red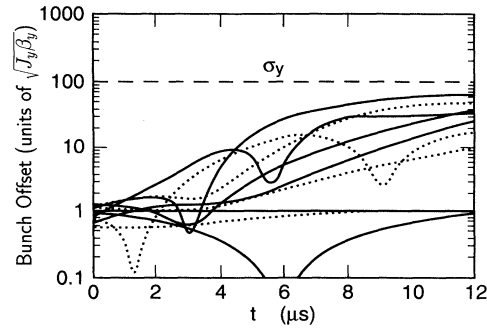uced by roughly a factor 2. For longer bunch trains, where the factor $\omega_{i0}l/c$ becomes larger, the reduction of the growth rate should be more pronounced. We should also note that we have characterized the instability with an approximate e-folding time τ_{growth}. While this differs from the characteristic time τ that more accurately describes the instability, which grows as $\exp(\sqrt{t/\tau})$, it provides a more intuitive estimate of the impact of the instability. For example, in the PEP-II HER, τ_{growth} is roughly 150 μs while $\tau \approx 6$ μs. This growth rate could be decreased further by adding additional clearing gaps in the bunch train [1]. For example, a second gap will increase the instability rise time to roughly $\tau_{\mathrm{growth}} \approx 0.6$ ms, which is inside the bandwidth of the feedback system.

Finally, our analytical model is confirmed by comparison with a macroparticle computer simulation and shows good agreement. An important effect that is not included in the model but will also suppress the instability is the tune spread in the electron beam. The tune spread can arise from the beam energy spread and the chromaticity of the optical lattice, the nonlinearity of the lattice, the space charge force due to the ions or the electrons themselves, or the beam-beam collision in a colliding beam storage ring. For example, in the PEP-II High Energy Ring with a beam-beam collision parameter $\xi = 0.03$, the estimated decoherence time for the betatron oscillations is 200 μs and is comparable with the growth rate of the instability.

ACKNOWLEDGMENTS

[1] T. O. Raubenheimer and F. Zimmermann, preceding paper, Phys. Rev. E **52**, 5487 (1995).

[2] PEP-II Report No. SLAC-418, 1993 (unpublished).

[3] Parameters for the NLC Damping Ring can be found in Report No. SLAC-436 (1994) (unpublished).

[4] R. E. Meller et al., Report No. SSC-N-360 (1987) (unpublished).